

5'-Terminal nucleotide variations in human cytoplasmic tRNA^{HisGUG} and its 5'-halves

MEGUMI SHIGEMATSU and YOHEI KIRINO

Computational Medicine Center, Sidney Kimmel Medical College, Thomas Jefferson University, Philadelphia, Pennsylvania 19107, USA

ABSTRACT

Transfer RNAs (tRNAs) are fundamental adapter components of translational machinery. tRNAs can further serve as a source of tRNA-derived noncoding RNAs that play important roles in various biological processes beyond translation. Among all species of tRNAs, tRNA^{HisGUG} has been known to uniquely contain an additional guanosine residue at the -1 position (G_{-1}) of its 5'-end. To analyze this -1 nucleotide in detail, we developed a TaqMan qRT-PCR method that can distinctively quantify human mature cytoplasmic tRNA^{HisGUG} containing G_{-1} , U_{-1} , A_{-1} , or C_{-1} or lacking the -1 nucleotide (starting from G_1). Application of this method to the mature tRNA fraction of BT-474 breast cancer cells revealed the presence of tRNA^{HisGUG} containing U_{-1} as well as the one containing G_{-1} . Moreover, tRNA lacking the -1 nucleotide was also detected, thus indicating the heterogeneous expression of 5'-tRNA^{HisGUG} variants. A sequence library of sex hormone-induced 5'-tRNA halves (5'-SHOT-RNAs), identified via cP-RNA-seq of a BT-474 small RNA fraction, also demonstrated the expression of 5'-tRNA^{HisGUG} halves containing G_{-1} , U_{-1} , or G_1 as 5'-terminal nucleotides. Although the detected 5'-nucleotide species were identical, the relative abundances differed widely between mature tRNA and 5'-half from the same BT-474 cells. The majority of mature tRNAs contained the -1 nucleotide, whereas the majority of 5'-halves lacked this nucleotide, which was biochemically confirmed using a primer extension assay. These results reveal the novel identities of tRNA^{HisGUG} molecules and provide insights into tRNA^{HisGUG} maturation and the regulation of tRNA half production.

Keywords: tRNA; tRNA^{HisGUG}; tRNA half; SHOT-RNA; -1 nucleotide

INTRODUCTION

Transfer RNAs (tRNAs) are noncoding RNAs (ncRNAs) with lengths of 60- to 90-nucleotide (nt) that play central roles as adapter molecules in the translational machinery. Although tRNA molecules are stable and abundant, the expression profiles of individual tRNAs vary dynamically among different cells and tissues (Dittmar et al. 2006; Pavon-Eternod et al. 2009; Zhou et al. 2009; Mahlab et al. 2012) and this variation has been implicated in the translational regulation of mRNA expression (Gingold et al. 2014), animal development (Marshall et al. 2012; Rideout et al. 2012; Schmitt et al. 2014), and disease (Daly et al. 2005; Pavon-Eternod et al. 2010; Zhou et al. 2012; Clarke et al. 2016). Accumulating evidence regarding tRNA-derived ncRNAs has further increased the complexity of tRNA biology. In many organisms, tRNAs are not always end products but are processed further into smaller ncRNAs, many of which are known to be functional molecules with roles in various biological processes beyond translation (Garcia-Silva et al. 2012; Gebetsberger and Polacek 2013; Anderson and Ivanov 2014; Saikia and

Hatzoglou 2015; Shigematsu and Kirino 2015; Telonis et al. 2015; Diebel et al. 2016). These tRNA-derived ncRNAs are in general classified into two groups: tRNA halves that range either from the 5'-end to the anticodon loop (5'-half) or from the anticodon loop to the 3'-end (3'-half) of a mature tRNA, and shorter tRNA-derived fragments (tRFs) that originate from various regions of mature tRNAs or their precursor transcripts (pre-tRNAs).

To date, two distinct classes of tRNA halves have been identified: tRNA-derived stress-induced RNAs (tiRNAs) (Thompson et al. 2008; Fu et al. 2009; Hsieh et al. 2009; Yamasaki et al. 2009; Saikia et al. 2012) and sex hormone-dependent tRNA-derived RNAs (SHOT-RNAs) (Honda et al. 2015). Although both tiRNAs and SHOT-RNAs are produced from mature tRNAs via angiogenin (ANG)-mediated cleavage of the anticodon loop (Fu et al. 2009; Yamasaki et al. 2009; Honda et al. 2015), the molecular factors that trigger their production are different. The expression of tiRNAs

Corresponding author: Yohei.Kirino@jefferson.edu

Article is online at <http://www.rnajournal.org/cgi/doi/10.1261/rna.058024.116>.

© 2017 Shigematsu and Kirino This article is distributed exclusively by the RNA Society for the first 12 months after the full-issue publication date (see <http://rnajournal.cshlp.org/site/misc/terms.xhtml>). After 12 months, it is available under a Creative Commons License (Attribution-NonCommercial 4.0 International), as described at <http://creativecommons.org/licenses/by-nc/4.0/>.

is triggered by a variety of stress stimuli, including oxidative stress, heat/cold shock, and UV irradiation (Shigematsu et al. 2014; Saikia and Hatzoglou 2015). The accumulation of tRNAs has been implicated in stress granule formation (Emara et al. 2010; Lyons et al. 2016), translational regulation (Yamasaki et al. 2009; Ivanov et al. 2011), and the pathogenesis of neurodevelopmental disorders (Blanco et al. 2014). In contrast, the expression of SHOT-RNAs is promoted by signaling pathways associated with sex hormones (e.g., estrogen and androgen) and their receptors (e.g., estrogen receptor [ER] and androgen receptor [AR]). SHOT-RNAs are specifically expressed in ER- or AR-positive breast and prostate cancers and have functional significance in cell proliferation (Honda et al. 2015).

Because ANG leaves a 2',3'-cyclic phosphate (cP) on its 5'-cleavage products (Shapiro et al. 1986), ANG-generated 5'-tRNA halves contain a cP at the 3'-end (Honda et al. 2015). These cP-containing RNAs cannot be captured accurately by standard RNA-seq methods because they are not ligated to a 3'-adapter during library preparation procedure. We circumvented the issue by developing a cP-RNA-seq method that can exclusively sequence cP-containing RNAs (Honda et al. 2015, 2016) and used this method to determine the expression repertoire of 5'-SHOT-RNAs (5'-tRNA halves) in human BT-474 ER-positive breast cancer cells; accordingly, we identified eight cytoplasmic (cyto) tRNA species as the major sources of SHOT-RNAs (Honda et al. 2015). Although 5'-SHOT-RNAs from cyto tRNA^{LysCUU} and tRNA^{HisGUG} were particularly enriched, the molecular mechanism by which specific tRNAs are selectively cleaved for SHOT-RNA production remains elusive.

Among all species of tRNAs, tRNA^{HisGUG} is unique in that it contains an additional guanosine residue at the -1 position (G_{-1}) of its 5'-end (Sprinzl et al. 1998). This G_{-1} residue is conserved across phyla and has been observed in bacteria (Singer and Smith 1972; Orellana et al. 1986), yeast (Keith and Pixa 1984), fruit fly (Altwegg and Kubli 1980), and mammals (Boisnard and Petrissant 1981; Rosa et al. 1983). In *Escherichia coli*, this G_{-1} residue is genome-encoded, and anomalous RNase P cleavage of pre-tRNA^{HisGUG} between positions -1 and -2 yields G_{-1} -containing tRNA^{HisGUG} (Orellana et al. 1986; Burkard et al. 1988). In yeast, G_{-1} is not derived from the genomic sequence; instead, tRNA^{His} guanylyltransferase (Thg1) post-transcriptionally adds this residue to the 5'-end (Gu et al. 2003). The conservation of G_{-1} residue addition via different mechanisms in different organisms implies the functional significance of the G_{-1} residue. Indeed, the G_{-1} residue is a critical determinant for the aminoacylation of tRNA^{HisGUG} by the cognate histidyl-tRNA synthetase (HisRS) in both *E. coli* (Himeno et al. 1989) and yeast (Rudinger et al. 1994; Rosen et al. 2006). In yeast, the loss of this G_{-1} residue consequent to the depletion of Thg1 or its polymerase activity causes a severe reduction in the tRNA^{HisGUG} aminoacylation levels, resulting in growth

impairment (Gu et al. 2005; Jackman and Phizicky 2008; Preston and Phizicky 2010). The G_{-1} residue is also implicated in post-transcriptional nucleotide modification because yeast lacking this residue has been shown to acquire additional 5-methylcytidine (m^5C) modifications (Gu et al. 2005; Preston et al. 2013), although a biological role for the interplay between the absence of G_{-1} and the presence of m^5C is unknown. In contrast to the presence and significance of G_{-1} in these studies, some organisms such as α -proteobacteria (Wang et al. 2007; Jackman et al. 2012), *Acanthamoeba* (Rao et al. 2013), and *Trypanosoma* (Rao and Jackman 2015) lack G_{-1} . HisRS does not require G_{-1} for aminoacylation in these species.

Despite the advent of next-generation sequencing (NGS) technologies and their widespread use in RNA-seq for transcriptome analyses, the -1 nucleotide of tRNA^{HisGUG} has not been investigated in RNA-seq-based studies. This could be partly attributable to the expectation that tRNA^{HisGUG} contains post-transcriptional modifications that would interfere with reverse transcription (Kellner et al. 2010), such as a 1-methyl-guanosine at nucleotide position 37 (m^1G_{37}) (Boisnard and Petrissant 1981) (nucleotide position [np] is based on the tRNA numbering system [Sprinzl et al. 1998]). Indeed, human and *Bombyx* 3'-halves of cyto tRNA^{HisGUG}, possessing G_{37} (likely modified to m^1G_{37}), could not be amplified by RT-PCR despite being successfully detected by Northern blot (Honda et al. 2015). The presence of the RT-interfering modification would lead to underrepresentation and bias in the tRNA^{HisGUG} sequence information generated from RNA-seq data. While analyzing a cP-RNA-seq library of 5'-SHOT-RNAs from BT-474 cells (Honda et al. 2015), we reasoned that this library would be useful for observing the -1 nucleotide on human cyto tRNA^{HisGUG} for the following reasons. First, 5'-SHOT-RNA^{HisGUG} (5'-half of cyto tRNA^{HisGUG}) does not contain RT-inhibitory modifications, and therefore sequence analyses should not be biased by modifications. Second, 5'-SHOT-RNA^{HisGUG} is produced from mature aminoacylated cyto tRNA^{HisGUG}, and therefore information about the -1 nucleotide in mature tRNA might be retained in this 5'-half. Third, 5'-SHOT-RNA^{HisGUG} was the second most abundant species in the 5'-SHOT-RNA library from BT-474 cells, and thereby sufficient sequence reads of the 5'-half are available for an estimation of the -1 nucleotide state.

In this study, we investigated the 5'-terminal nucleotides of 5'-SHOT-RNA^{HisGUG} expressed in human BT-474 cells and observed an unexpected level of variation that was not limited to G_{-1} . Furthermore, we developed a TaqMan qRT-PCR-based method that could distinctively quantify each tRNA variant containing a different 5'-terminal nucleotide and thus clarified a 5'-terminal nucleotide variation of the mature cyto tRNA^{HisGUG} expressed in the same BT-474 cells. This identification and comparison of the 5'-terminal nucleotides and their variations among mature cyto tRNA^{HisGUG} and 5'-half molecules have yielded insights

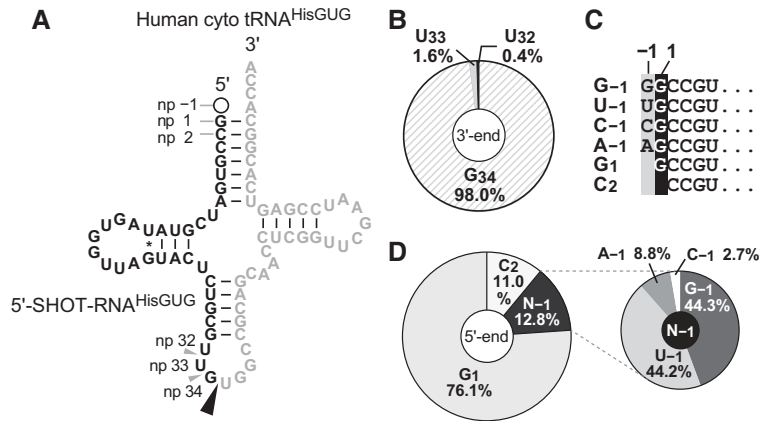


FIGURE 1. Terminal nucleotide analyses of BT-474 5'-SHOT-RNA^{HisGUG} identified by cP-RNA-seq. (A) The cloverleaf secondary structure of the major isodecoder of human cyto tRNA^{HisGUG} encoded by nine genes (Supplemental Fig. S1) on the genome. Nucleotide positions (np) are indicated according to the tRNA nucleotide numbering systems (Sprinzl et al. 1998). The ANG-cleavage sites for SHOT-RNA production, predicted by the 3'-terminal position of 5'-SHOT-RNA^{HisGUG}, are indicated by arrowheads. Regions from which 5'-SHOT-RNA^{HisGUG} molecules were derived are shown in black; other regions are shown in gray. (B) Pie chart indicating the 3'-terminal position of 5'-SHOT-RNA^{HisGUG}. (C) The six 5'-terminal variations identified in 5'-SHOT-RNA^{HisGUG}. (D) Pie charts showing the 5'-terminal positions of 5'-SHOT-RNA^{HisGUG}.

into tRNA^{HisGUG} identities and the regulatory mechanisms underlying tRNA^{HisGUG} maturation and cleavage.

RESULTS AND DISCUSSION

The majority of 5'-SHOT-RNA^{HisGUG} molecules lack the -1 nucleotide

The human nuclear genome contains 11 cyto tRNA^{HisGUG} genes that encode three different isodecoders (Supplemental Fig. S1). In the 5'-SHOT-RNA sequence repertoire of BT-474 cells, which was previously identified using cP-RNA-seq (Honda et al. 2015, 2016), 5'-SHOT-RNA^{HisGUG} sequences constituted approximately 7.9 million reads, comprising 27.5% of the total reads of 5'-SHOT-RNAs. Accordingly, 5'-SHOT-RNA^{HisGUG} is the second most abundant 5'-SHOT-RNA species in BT-474 cells, after 5'-SHOT-RNA^{LysCUU}. Almost all of the identified 5'-SHOT-RNA^{HisGUG} sequences corresponded to a single major isodecoder of cyto tRNA^{HisGUG} (Fig. 1A) that is encoded by nine of the 11 genes (Supplemental Fig. S1), suggesting that this isodecoder is the major cyto tRNA^{HisGUG} molecule expressed in the cells. Almost all (98%) of the 5'-SHOT-RNA^{HisGUG} had a 3'-terminal position at np 34 (Fig. 1B), indicating a focal pattern of ANG cleavage between the anticodon first (G₃₄) and second (U₃₅) letters during the production of 5'-SHOT-RNA^{HisGUG}. In contrast to the consistent 3'-termini, six 5'-terminal variations were observed among the sequenced 5'-SHOT-RNA^{HisGUG} (Fig. 1C). In contrast to previous reports of a major presence of the 5'-terminal G₋₁ in tRNA^{HisGUG}, a majority (>75%) of 5'-SHOT-RNA^{HisGUG} lacked the -1 nucleotide and initiated at np 1 (G₁) (Fig.

1D). The second most abundant class (>12%) of 5'-SHOT-RNA^{HisGUG} contained the -1 nucleotide; here, both guanosine (G₋₁; 44.3%) and uridine (U₋₁; 44.2%) were frequently present at the -1 nucleotide. The other two nucleotides (A₋₁; 9%; C₋₁; 3%) were also detected as minor -1 nucleotide species, and a 5'-SHOT-RNA^{HisGUG} initiating from np 2 (C₂; 11%) was also identified.

Experimental validation of the predominant expression of 5'-SHOT-RNA^{HisGUG} lacking the -1 nucleotide

Because our cP-RNA-seq scheme includes several chemical and enzymatic RNA treatments (Honda et al. 2015, 2016), unexpected variations of the 5'-termini of 5'-SHOT-RNA^{HisGUG} might have resulted from undesired procedural RNA damage. To exclude this possibility and confirm that our cP-RNA-seq results

reflect the cellular state of RNA expression, we conducted a primer extension assay for 5'-SHOT-RNA^{HisGUG}. In this assay, a radiolabeled DNA primer complementary to np 6–25 of cyto tRNA^{HisGUG} (Fig. 2A) was specifically hybridized to 5'-SHOT-RNA^{HisGUG} present in gel-purified small RNA fractions (20–50 nt) from BT-474 cells; subsequently, reverse transcription was carried out from the primer. When using synthetic tRNA^{HisGUG} initiating from G₁ as a template, the 5-nt primer extension was detected as a 25-nt band (Fig. 2B). In contrast, the use of synthetic tRNA^{HisGUG} containing G₋₁ yielded an additional extension of 1 nt and a 26-nt band that was clearly distinct from the above-mentioned 25-nt band. An equal mix of these two synthetic tRNAs yielded two bands of equal abundance, indicating the ability of this assay to estimate the presence or absence of the -1 nucleotide. By performing reactions using dideoxynucleotides, we confirmed that the reverse transcription was correctly run on tRNA^{HisGUG} in both synthetic RNA and cellular RNA samples (Supplemental Fig. S2). Analyses of BT-474 small RNA fractions revealed the marked and more abundant presence of the 25-nt band in comparison with the 26-nt band (Fig. 2B). Quantification of the band intensities suggested that ~70% of the 5'-SHOT-RNA^{HisGUG} lacks the -1 nucleotide (Supplemental Fig. S3), which is consistent with the cP-RNA-seq-based analyses shown in Figure 1. These results indicate that the majority of the 5'-SHOT-RNA^{HisGUG} molecules expressed in BT-474 cells lack the -1 nucleotide and initiate from G₁. In the primer extension assay, we did not observe a clear 24-nt band corresponding to 5'-SHOT-RNA^{HisGUG} initiating from C₂; therefore, the presence of such RNA in cP-RNA-seq data might result from undesired procedural RNA damage.

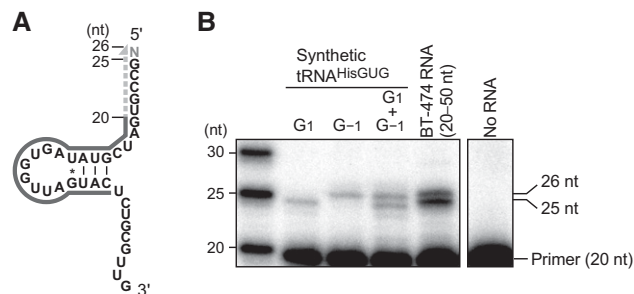


FIGURE 2. Primer extension assay to determine the 5'-terminal position of 5'-SHOT-RNA^{HisGUG}. (A) The cloverleaf secondary structure of 5'-SHOT-RNA^{HisGUG} used as a primer extension template. The 5'-end-labeled 20-nt primer, which was hybridized to the D-arm of tRNA, is shown as a black solid line; nascent cDNA synthesized from the primer is indicated as a gray dotted line. Reverse transcription from the primer terminates at np 1 or -1 to yield a cDNA band with a length of 25 or 26 nt, respectively. (B) Synthetic mature tRNA^{HisGUG} containing either G₁ or G₋₁, or a 30- to 50-nt small RNA fraction of BT-474 cells were subjected to a primer extension assay for an analysis of the 5'-terminal position of 5'-SHOT-RNA^{HisGUG}. An assay without template RNA was also performed as a negative control experiment.

Development of a TaqMan qRT-PCR-based method for the discriminative quantification of 5'-terminal variants of mature cyto tRNA^{HisGUG}

SHOT-RNAs originate from mature aminoacylated tRNAs (Honda et al. 2015); accordingly, we reasoned that the 5'-terminal variations of 5'-SHOT-RNA^{HisGUG} would mirror those of mature cyto tRNA^{HisGUG}, although these variations did not match the canonical, reported variations in mature tRNA. Because RNA-seq data are not appropriate for analyses of mature tRNA^{HisGUG} sequences, we developed a TaqMan qRT-PCR-based method that can discriminatively quantify each 5'-terminal variant of mature cyto tRNA^{HisGUG} containing G₋₁, U₋₁, A₋₁, C₋₁, or G₁ as the 5'-terminal nucleotide. We focused on a single major isodecoder encoded by nine of 11 genes in the human genome (Supplemental Fig. S1).

In the developed method, mature tRNA fractions (70–90 nt) were first gel-purified from total RNA, after which an acceptor-stem disrupter (AS-disrupter), a DNA oligo complementary to np 55–76 (3'-end) of the cyto tRNA^{HisGUG}, was hybridized to the purified fractions (Fig. 3A,B; Supplemental Fig. S4). Subsequently, a DNA/RNA chimeric 5'-adapter was ligated to the 5'-ends of mature tRNA^{HisGUG}, and the ligation product was amplified and quantified by TaqMan qRT-PCR to eventually generate an 86- (tRNA starting from G₁) or 87-bp cDNA (tRNA containing -1 nucleotide). The AS-disrupter was utilized to disrupt mature tRNA^{HisGUG} structure; this disruption was expected to enhance the accessibility of the adapter, primer, and enzymes to the tRNA and thereby increase the reaction efficiencies following hybridization. In addition, dimethyl sulfoxide (DMSO) and polyethylene glycol (PEG) 8000, both of which enhance RNA ligation efficiency, were added to the adapter ligation reaction. Indeed, the combined inclusion of the

AS-disrupter hybridization step and addition of PEG/DMSO to the ligation reaction increased the detection efficiency of synthetic tRNA^{HisGUG} with G₋₁ by more than 95-fold and prevented the synthesis of nonspecific cDNA bands (Fig. 3C). The TaqMan probe was designed to target the boundary of the adapter and the 5'-end of mature tRNA^{HisGUG}, thus allowing an exclusive analysis of the tRNA 5'-end in the ligation product. Indeed, we were unable to detect an amplification signal in the absence of T4 RNA ligase (Fig. 3C). Because the TaqMan probe has a single-nucleotide resolution (Ranade et al. 2001; Honda and Kirino 2015), our design scheme was expected to distinctively quantify each 5'-terminal variant of tRNA^{HisGUG} without cross-reactivity with other variant species. We confirmed the exclusive specificity of our TaqMan probes to quantify perfectly matched target sequences without cross-reactivity from other variants (Supplemental Table S1). To examine the quantification ability, our method was applied to different amounts of synthetic mature tRNA^{HisGUG} (0.1–100 fmol). To mimic tRNA quantification using a total tRNA fraction, an *E. coli* tRNA fraction was mixed with synthetic RNA as a carrier; we confirmed that the *E. coli* tRNA fraction did not yield an amplification signal in our system. For all five synthetic 5'-terminal variants, the quantifications demonstrated clear linearity between the log of tRNA input and the *Ct* value (Supplemental Fig. S5), indicating that this method has a dynamic range of at least three orders of magnitude, and discriminatively quantifies the 5'-terminal variants. We further validated our method by quantifying a mixture of different synthetic tRNA variants. Since 5'-SHOT-RNAs^{HisGUG} starting from G₁, G₋₁, and U₋₁ were mainly detected (Fig. 1D), corresponding mature synthetic tRNAs^{HisGUG} were mixed at several different ratios and subjected to the method with an *E. coli* tRNA carrier. The amount of each detected tRNA was calculated based on the standard curves (Supplemental Fig. S5). As shown in Figure 3D, the resultant relative abundances of detected tRNAs well reflected those of the tRNAs added to the reactions, allowing us to conclude that our method can estimate the relative abundance of 5'-terminal variants of mature tRNA^{HisGUG}.

The majority of the mature tRNA^{HisGUG} molecules contain the -1 nucleotide

Given the high specificity and quantification ability of our TaqMan qRT-PCR method, we utilized this method to determine the relative abundances of the 5'-terminal variants of endogenous mature cyto tRNA^{HisGUG} expressed in BT-474 cells. Using our synthetic tRNA results as standards, we determined the relative abundances of the five potential 5'-terminal variants of tRNA^{HisGUG}. In contrast to the 5'-terminal variations of 5'-SHOT-RNA^{HisGUG}, which were dominated by G₁ (Fig. 1C), ~60% of the mature tRNA^{HisGUG} contained G₋₁ as a 5'-terminal nucleotide (Fig. 4A). A significant proportion of tRNAs contained U₋₁ (~20%), and a similar

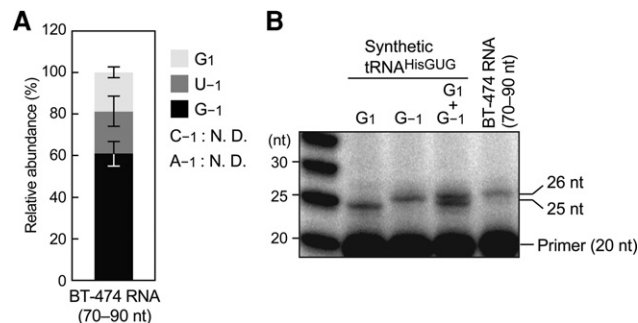


FIGURE 4. Variations in 5'-terminal nucleotide from mature tRNA^{HisGUG} expressed in BT-474 cells. (A) Of note, 70- to 90-nt mature tRNA fractions of BT-474 cells were subjected to TaqMan qRT-PCR quantification of each 5'-terminal variant of mature tRNA^{HisGUG}. Expression levels were estimated using standard curves from synthetic tRNAs (Supplemental Fig. S5), and the relative abundances of mature tRNAs containing each 5'-terminal nucleotide are shown. Bars indicate SD from three independent experiments. N.D. indicates that the reaction did not amplify detectable cDNA signals. (B) A primer extension assay to analyze the 5'-terminal positions of mature tRNA^{HisGUG} was performed using the 70- to 90-nt mature tRNA fraction from BT-474 cells.

cell lines. The mechanism underlying the formation of these 5'-variations in mature tRNA and the functional significance remain to be determined. Because Thg1 or a Thg1-like protein (TLP) from *Bacillus*, archaea and yeast can attach not only to guanosine, but also to uridine, to the -1 position of the tRNA in vitro (Jackman and Phizicky 2006; Rao et al. 2011), Thg1 might incorporate both G $_{-1}$ and U $_{-1}$ into human mature tRNA^{HisGUG}. It will be intriguing to analyze the efficiency of human HisRS aminoacylation toward each mature tRNA^{HisGUG} 5'-variant to determine whether these variations affect the regulation of aminoacylation. Because human Thg1 is associated with cell cycle regulation (Guo et al. 2004), the biological significance of these 5'-variations in mature tRNA^{HisGUG} might also include cell growth regulation.

The 5'-terminal variations of 5'-SHOT-RNA^{HisGUG} exhibited a pattern distinct from that of mature tRNA; specifically, 5'-SHOT-RNA^{HisGUG} molecules mostly lack the -1 nucleotide. This inconsistency might be attributable to ANG cleavage activity to generate SHOT-RNAs. ANG might selectively cleave -1 nucleotide-lacking tRNAs, resulting in a considerable accumulation of -1 nucleotide-lacking SHOT-RNA molecules. However, ANG is a small protein, and thus selective cleavage should be facilitated by cofactors. Alternatively, ANG might cleave tRNA irrespective of the 5'-terminal nucleotide; SHOT-RNA lacking the -1 nucleotide might then be more stable within the cells than SHOT-RNA containing G $_{-1}$, or an unknown ribonuclease might trim the -1 nucleotide from SHOT-RNAs. The generative mechanism and biological significance of these 5'-terminal variations in mature tRNA^{HisGUG} molecules 5'-halves remain to be elucidated.

MATERIALS AND METHODS

Bioinformatics analyses of 5'-SHOT-RNA^{HisGUG}

Human cyto tRNA^{HisGUG} sequences were identified using the tRNAscan-SE program (Lowe and Eddy 1997) and are shown in Supplemental Figure S1. The 5'-SHOT-RNA library was previously obtained by cP-RNA-seq of gel-purified 30- to 50-nt RNAs from BT-474 cells (Honda et al. 2015) and can be found in the Gene Expression Omnibus Database (GEO accession no. SRX1060214). Reads previously mapped to mature cyto tRNA^{HisGUG} sequences (Honda et al. 2015) were extracted and used for this study.

Cell culture

BT-474 cells were cultured in Dulbecco's modified Eagle's medium (DMEM; Life Technologies) containing 10% (v/v) FBS.

In vitro synthesis of tRNA^{HisGUG}

Templates for the in vitro synthesis of human cyto tRNA^{HisGUG} (with or without N $_{-1}$ nucleotide) were prepared by annealing two ssDNAs (5'-GCTTAATACGACTCACTATAGCCGTGATCGTATA GTGGTTAGTACTCTGCGTTGTGGC-3' and 5'-mUmGGTGCC GTGACTCGGATTCTGAACCGAGGTTGCTGCGGCCACAACGC-3') in a solution containing 10 mM Tris-HCl (pH 8.0) and 20 mM MgCl₂. After blunting the formed duplex using sequenase (Affymetrix), the resultant dsDNAs were used as templates for transcription with T7 RNA polymerase (New England Biolabs). Synthesized RNAs were gel-purified using denaturing PAGE.

5'-End identification of tRNA^{HisGUG} by TaqMan qRT-PCR

The sequences of the adapter, AS-disrupter, primers, and TaqMan probes for TaqMan qRT-PCR are shown in Supplemental Table S4. The 70- to 90-nt RNA fraction, which contained mature tRNAs, was initially gel-purified from total RNA using denaturing PAGE. To ligate the 5'-adapter, to the 5'-end of cyto tRNA^{HisGUG}, 500 ng of the tRNA fraction were incubated with 100 pmol of AS-disrupter in a 4- μ L reaction mixture at 90°C for 2 min and subsequently incubated at 37°C. RNA was then added immediately to a ligation reaction mixture (total volume: 10 μ L) containing 200 pmol of 5'-adapter, T4 RNA ligase 1 (New England Biolabs), 10% (v/v) DMSO, and 5% PEG8000 and incubated at 37°C for 1 h, followed by an overnight incubation at 4°C. Next, 1 μ L of the ligation mixture was subjected to cDNA synthesis with 1 μ M of RT primer and SuperScript III (Invitrogen). For TaqMan qPCR quantification, the cDNA product (0.5 μ L of the RT mixture) was added to a reaction mixture (total volume: 10 μ L) containing 5 μ L of qPCR Master Mix (TaKaRa), 0.2 μ M each of reverse and forward primers, and 0.1 μ M of TaqMan probe. Using a StepOne Plus Real-time PCR machine (Applied Biosystems), the reaction mixture was incubated at 95°C for 20 sec, followed by 40 cycles of 95°C for 1 sec and 65°C for 20 sec.

Primer extension assay

To detect 5'-SHOT-RNA^{HisGUG}, 30- to 50-nt RNAs were first gel-purified from BT-474 total RNA. Subsequently, 50 ng of gel-purified

RNA or 0.1 pmol of synthetic tRNA^{HisGUG} were incubated with SuperScript III, the corresponding reaction buffer (Invitrogen), and 0.1 pmol of 5'-³²P-labeled DNA primer (5'-GTACTAACCCATATACGATC-3') at 55°C for 30 min. The reaction mixtures were developed using denaturing PAGE containing 7 M urea and 20% formamide. To analyze mature tRNA^{HisGUG}, 70- to 90-nt mature tRNAs were gel-purified from the total RNAs extracted from BT-474 cells. Gel-purified RNAs (1 µg) were then subjected to a primer extension assay as described above.

SUPPLEMENTAL MATERIAL

Supplemental material is available for this article.

ACKNOWLEDGMENTS

We are grateful to Dr. Shozo Honda for helpful discussions. This study was supported by National Institutes of Health, National Institute of General Medical Sciences grant GM106047 (to Y.K.).

Received June 22, 2016; accepted November 18, 2016.

REFERENCES

- Altwegg M, Kubli E. 1980. The nucleotide sequence of histidine tRNA γ of *Drosophila melanogaster*. *Nucleic Acids Res* **8**: 3259–3262.
- Anderson P, Ivanov P. 2014. tRNA fragments in human health and disease. *FEBS Lett* **588**: 4297–4304.
- Blanco S, Dietmann S, Flores JV, Hussain S, Kutter C, Humphreys P, Lukk M, Lombard P, Treps L, Popis M, et al. 2014. Aberrant methylation of tRNAs links cellular stress to neuro-developmental disorders. *EMBO J* **33**: 2020–2039.
- Boisnard M, Petrissant G. 1981. The nucleotide sequence of sheep liver histidine-tRNA (anticodon Q-U-G). *FEBS Lett* **129**: 180–184.
- Burkard U, Willis I, Söll D. 1988. Processing of histidine transfer RNA precursors. Abnormal cleavage site for RNase P. *J Biol Chem* **263**: 2447–2451.
- Clarke CJ, Berg TJ, Birch J, Ennis D, Mitchell L, Cloix C, Campbell A, Sumpton D, Nixon C, Campbell K, et al. 2016. The initiator methionine tRNA drives secretion of type II collagen from stromal fibroblasts to promote tumor growth and angiogenesis. *Curr Biol* **26**: 755–765.
- Daly NL, Arvanitis DA, Fairley JA, Gomez-Roman N, Morton JP, Graham SV, Spandidos DA, White RJ. 2005. Deregulation of RNA polymerase III transcription in cervical epithelium in response to high-risk human papillomavirus. *Oncogene* **24**: 880–888.
- Diebel KW, Zhou K, Clarke AB, Bemis LT. 2016. Beyond the ribosome: extra-translational functions of tRNA fragments. *Biomark Insights* **11**: 1–8.
- Dittmar KA, Goodenbour JM, Pan T. 2006. Tissue-specific differences in human transfer RNA expression. *PLoS Genet* **2**: e221.
- Emara MM, Ivanov P, Hickman T, Dawra N, Tisdale S, Kedersha N, Hu GF, Anderson P. 2010. Angiogenin-induced tRNA-derived stress-induced RNAs promote stress-induced stress granule assembly. *J Biol Chem* **285**: 10959–10968.
- Fu H, Feng J, Liu Q, Sun F, Tie Y, Zhu J, Xing R, Sun Z, Zheng X. 2009. Stress induces tRNA cleavage by angiogenin in mammalian cells. *FEBS Lett* **583**: 437–442.
- Garcia-Silva MR, Cabrera-Cabrera F, Güida MC, Cayota A. 2012. Hints of tRNA-derived small RNAs role in RNA silencing mechanisms. *Genes (Basel)* **3**: 603–614.
- Gebetsberger J, Polacek N. 2013. Slicing tRNAs to boost functional ncRNA diversity. *RNA Biol* **10**: 1798–1806.
- Gingold H, Tehler D, Christoffersen NR, Nielsen MM, Asmar F, Kooistra SM, Christophersen NS, Christensen LL, Borre M, Sorensen KD, et al. 2014. A dual program for translation regulation in cellular proliferation and differentiation. *Cell* **158**: 1281–1292.
- Gu W, Jackman JE, Lohan AJ, Gray MW, Phizicky EM. 2003. tRNA^{His} maturation: an essential yeast protein catalyzes addition of a guanine nucleotide to the 5' end of tRNA^{His}. *Genes Dev* **17**: 2889–2901.
- Gu W, Hurto RL, Hopper AK, Grayhack EJ, Phizicky EM. 2005. Depletion of *Saccharomyces cerevisiae* tRNA^{His} guanylyltransferase Thg1p leads to uncharged tRNA^{His} with additional m⁶C. *Mol Cell Biol* **25**: 8191–8201.
- Guo D, Hu K, Lei Y, Wang Y, Ma T, He D. 2004. Identification and characterization of a novel cytoplasm protein ICF45 that is involved in cell cycle regulation. *J Biol Chem* **279**: 53498–53505.
- Himeno H, Hasegawa T, Ueda T, Watanabe K, Miura K, Shimizu M. 1989. Role of the extra G-C pair at the end of the acceptor stem of tRNA^{His} in aminoacylation. *Nucleic Acids Res* **17**: 7855–7863.
- Honda S, Kirino Y. 2015. Dumbbell-PCR: a method to quantify specific small RNA variants with a single nucleotide resolution at terminal sequences. *Nucleic Acids Res* **43**: e77.
- Honda S, Loher P, Shigematsu M, Palazzo JP, Suzuki R, Imoto I, Rigoutsos I, Kirino Y. 2015. Sex hormone-dependent tRNA halves enhance cell proliferation in breast and prostate cancers. *Proc Natl Acad Sci* **112**: E3816–E3825.
- Honda S, Morichika K, Kirino Y. 2016. Selective amplification and sequencing of cyclic phosphate-containing RNAs by the cP-RNA-seq method. *Nat Protoc* **11**: 476–489.
- Hsieh LC, Lin SI, Shih AC, Chen JW, Lin WY, Tseng CY, Li WH, Chiou TJ. 2009. Uncovering small RNA-mediated responses to phosphate deficiency in *Arabidopsis* by deep sequencing. *Plant Physiol* **151**: 2120–2132.
- Ivanov P, Emara MM, Villen J, Gygi SP, Anderson P. 2011. Angiogenin-induced tRNA fragments inhibit translation initiation. *Mol Cell* **43**: 613–623.
- Jackman JE, Phizicky EM. 2006. tRNA^{His} guanylyltransferase catalyzes a 3'-5' polymerization reaction that is distinct from G-1 addition. *Proc Natl Acad Sci* **103**: 8640–8645.
- Jackman JE, Phizicky EM. 2008. Identification of critical residues for G-1 addition and substrate recognition by tRNA^{His} guanylyltransferase. *Biochemistry* **47**: 4817–4825.
- Jackman JE, Gott JM, Gray MW. 2012. Doing it in reverse: 3'-to-5' polymerization by the Thg1 superfamily. *RNA* **18**: 886–899.
- Keith G, Pixa G. 1984. The nucleotide sequence of asparagine tRNA from brewer's yeast. *Biochimie* **66**: 639–643.
- Kellner S, Burhenne J, Helm M. 2010. Detection of RNA modifications. *RNA Biol* **7**: 237–247.
- Lowe TM, Eddy SR. 1997. tRNAscan-SE: a program for improved detection of transfer RNA genes in genomic sequence. *Nucleic Acids Res* **25**: 955–964.
- Lyons SM, Achorn C, Kedersha NL, Anderson PJ, Ivanov P. 2016. YB-1 regulates tRNA-induced stress granule formation but not translational repression. *Nucleic Acids Res* **44**: 6949–6960.
- Mahlab S, Tuller T, Linial M. 2012. Conservation of the relative tRNA composition in healthy and cancerous tissues. *RNA* **18**: 640–652.
- Marshall L, Rideout EJ, Grewal SS. 2012. Nutrient/TOR-dependent regulation of RNA polymerase III controls tissue and organismal growth in *Drosophila*. *EMBO J* **31**: 1916–1930.
- Orellana O, Cooley L, Söll D. 1986. The additional guanylate at the 5' terminus of *Escherichia coli* tRNA^{His} is the result of unusual processing by RNase P. *Mol Cell Biol* **6**: 525–529.
- Pavon-Eternod M, Gomes S, Geslain R, Dai Q, Rosner MR, Pan T. 2009. tRNA over-expression in breast cancer and functional consequences. *Nucleic Acids Res* **37**: 7268–7280.
- Pavon-Eternod M, Wei M, Pan T, Kleiman L. 2010. Profiling non-lysyl tRNAs in HIV-1. *RNA* **16**: 267–273.
- Preston MA, Phizicky EM. 2010. The requirement for the highly conserved G-1 residue of *Saccharomyces cerevisiae* tRNA^{His} can be circumvented by overexpression of tRNA^{His} and its synthetase. *RNA* **16**: 1068–1077.

- Preston MA, D'Silva S, Kon Y, Phizicky EM. 2013. tRNA^{His} 5-methylcytidine levels increase in response to several growth arrest conditions in *Saccharomyces cerevisiae*. *RNA* **19**: 243–256.
- Ranade K, Chang MS, Ting CT, Pei D, Hsiao CF, Olivier M, Pesich R, Hebert J, Chen YD, Dzau VJ, et al. 2001. High-throughput genotyping with single nucleotide polymorphisms. *Genome Res* **11**: 1262–1268.
- Rao BS, Jackman JE. 2015. Life without post-transcriptional addition of G-1: two alternatives for tRNA^{His} identity in Eukarya. *RNA* **21**: 243–253.
- Rao BS, Maris EL, Jackman JE. 2011. tRNA 5'-end repair activities of tRNA^{His} guanylyltransferase (Thg1)-like proteins from Bacteria and Archaea. *Nucleic Acids Res* **39**: 1833–1842.
- Rao BS, Mohammad F, Gray MW, Jackman JE. 2013. Absence of a universal element for tRNA^{His} identity in *Acanthamoeba castellanii*. *Nucleic Acids Res* **41**: 1885–1894.
- Rideout EJ, Marshall L, Grewal SS. 2012. *Drosophila* RNA polymerase III repressor Maf1 controls body size and developmental timing by modulating tRNA^{Met} synthesis and systemic insulin signaling. *Proc Natl Acad Sci* **109**: 1139–1144.
- Rosa MD, Hendrick JP, Lerner MR, Steitz JA, Reichlin M. 1983. A mammalian tRNA^{His}-containing antigen is recognized by the polymyositis-specific antibody anti-Jo-1. *Nucleic Acids Res* **11**: 853–870.
- Rosen AE, Brooks BS, Guth E, Francklyn CS, Musier-Forsyth K. 2006. Evolutionary conservation of a functionally important backbone phosphate group critical for aminoacylation of histidine tRNAs. *RNA* **12**: 1315–1322.
- Rudinger J, Florentz C, Giegé R. 1994. Histidylation by yeast HisRS of tRNA or tRNA-like structure relies on residues –1 and 73 but is dependent on the RNA context. *Nucleic Acids Res* **22**: 5031–5037.
- Saikia M, Hatzoglou M. 2015. The many virtues of tRNA-derived stress-induced RNAs (tiRNAs): discovering novel mechanisms of stress response and effect on human health. *J Biol Chem* **290**: 29761–29768.
- Saikia M, Krokowski D, Guan BJ, Ivanov P, Parisien M, Hu GF, Anderson P, Pan T, Hatzoglou M. 2012. Genome-wide identification and quantitative analysis of cleaved tRNA fragments induced by cellular stress. *J Biol Chem* **287**: 42708–42725.
- Schmitt BM, Rudolph KL, Karagianni P, Fonseca NA, White RJ, Talianidis I, Odom DT, Marioni JC, Kutter C. 2014. High-resolution mapping of transcriptional dynamics across tissue development reveals a stable mRNA-tRNA interface. *Genome Res* **24**: 1797–1807.
- Shapiro R, Riordan JF, Vallee BL. 1986. Characteristic ribonucleolytic activity of human angiogenin. *Biochemistry* **25**: 3527–3532.
- Shigematsu M, Kirino Y. 2015. tRNA-derived short non-coding RNA as interacting partners of argonaute proteins. *Gene Regul Syst Bio* **9**: 27–33.
- Shigematsu M, Honda S, Kirino Y. 2014. Transfer RNA as a source of small functional RNA. *J Mol Biol Mol Imaging* **1**: 8.
- Singer CE, Smith GR. 1972. Histidine regulation in *Salmonella typhimurium*. 13. Nucleotide sequence of histidine transfer ribonucleic acid. *J Biol Chem* **247**: 2989–3000.
- Sprinzel M, Horn C, Brown M, Ioudovitch A, Steinberg S. 1998. Compilation of tRNA sequences and sequences of tRNA genes. *Nucleic Acids Res* **26**: 148–153.
- Telonis AG, Loher P, Honda S, Jing Y, Palazzo J, Kirino Y, Rigoutsos I. 2015. Dissecting tRNA-derived fragment complexities using personalized transcriptomes reveals novel fragment classes and unexpected dependencies. *Oncotarget* **6**: 24797–24822.
- Thompson DM, Lu C, Green PJ, Parker R. 2008. tRNA cleavage is a conserved response to oxidative stress in eukaryotes. *RNA* **14**: 2095–2103.
- Wang C, Sobral BW, Williams KP. 2007. Loss of a universal tRNA feature. *J Bacteriol* **189**: 1954–1962.
- Yamasaki S, Ivanov P, Hu GF, Anderson P. 2009. Angiogenin cleaves tRNA and promotes stress-induced translational repression. *J Cell Biol* **185**: 35–42.
- Zheng G, Qin Y, Clark WC, Dai Q, Yi C, He C, Lambowitz AM, Pan T. 2015. Efficient and quantitative high-throughput tRNA sequencing. *Nat Methods* **12**: 835–837.
- Zhou Y, Goodenbour JM, Godley LA, Wickrema A, Pan T. 2009. High levels of tRNA abundance and alteration of tRNA charging by bortezomib in multiple myeloma. *Biochem Biophys Res Commun* **385**: 160–164.
- Zhou DH, Lee J, Frankenberger C, Geslain R, Rosner M, Pan T. 2012. Anti-tumor effects of an engineered “killer” transfer RNA. *Biochem Biophys Res Commun* **427**: 148–153.